FULL PAPER

Engineering Zeolitic-Imidazolate Framework (ZIF) Thin Film Devices for Selective Detection of Volatile Organic Compounds

*Min Tu, Suttipong Wannapaiboon, Kira Khaletskaya, and Roland A. Fischer**

Thin films of sodalite-type zeolitic-imidazolate frameworks (ZIFs, ZIF-7, 8, 9, 67, 90, and ZIF-65-Zn) with different metal centers and functional moieties are fabricated on SiO_2 coated quartz crystal microbalance (QCM) substrates using automatic program controlled repeated direct growth method. The repeated direct growth procedure manipulated here shows great applicability for rapid growth of uniform ZIF thin films with controllable thickness. The fabricated ZIF/QCM devices are used to detect vapor phase volatile organic compounds including alcohol/water, BTEX compounds (benzene, toluene, ethylbenzene and xylene isomers), and hexane isomers. The ZIF/QCM devices exhibit selective detection behavior upon exposure to these chemical vapors. The effects of ZIF pore size, limited pore diameter, surface functionality, and structural flexibility on the sensing performances of ZIF/QCM devices are systematically investigated, which would be beneficial for the practical application of ZIF sensors based on array-sensing technology. Furthermore, the selective adsorption behavior suggests that these ZIF materials have great potentials in the applications of biofuel recovery and the separation of benzene/cyclohexane, xylene, and hexane isomers.

1. Introduction

The detection of useful or toxic analytes has attracted great interest for a range of applications, including pharmacology, environmental monitoring, and industrial process management. It has been recognized that well-designed host structures are essential for sensitive and selective detection of chemicals. Recently, the application of a novel class of materials, metal-organic frameworks (MOFs), for chemical detection becomes matured.[1–3] MOFs are built from metal (or inorganic clusters) centers bridged by organic linkers through coordination bonds.[4] The structural diversity and the presence of both inorganic and organic components in MOFs enable tunable properties with respect to framework pore size/geometry and surface functionality. Some optimized structures could provide tunable responsiveness and switching properties in response to external stimuli (such as temperature, pressure, electric potential, acoustic waves, and chemical environment), leading to the selectivity and sensitivity to detect such particular analytes.[5–7] Generally, in order to employ MOFs for chemical detection (except those based on luminescence quenching),[3] some external means of signal transduction such as optical, electrical, and mechanical schemes have to be applied.[6–12] Thus, integrating MOFs as thin films on device surfaces is able to form a physical interface for signal transduction. As the change in oscillating frequency of quartz crystal microbalance (QCM) is directly related to the mass change on the surface,[13] it has shown its applicability in chemical detection coupling with MOF thin films.[14–18]

As a sub-class of MOFs, zeolitic-imidazolate frameworks (ZIFs) constructed by linking metal centers (e.g., Zn, Co, and Cd) with imidazolate ligands show high porosity, structure diversity, tunable surface functionality, structure flexibility, and especially, good chemical and thermal stability which are essential for realistic applications.[19–22] These interesting properties make them good candidates as host sensing materials.[23–26] For example, Lu and Hupp[25] fabricated ZIF-8 film on Fabry–Pérot device for gases and chemical vapors detection by monitoring the changes of refractive index upon adsorption of guest molecules. The repeated direct growth method they used for ZIF-8 film growth offers several advantages including mild growth condition, rapid growth rate, and good control of thickness. However, the method has not been extended to fabricate other functional ZIF thin films up to date. Integrating a range of different ZIFs into thin film devices on various surfaces remains a challenge with respect to various applications such as membrane based gas/liquid separation, electronic and opto-electronic devices.[8–12] Furthermore, the sensing performances not only depend on the quality of ZIF thin films but also strongly rely on the properties of host ZIF materials such as limited pore diameter (LPD), surface functionality, and structure flexibility. Thus, the systematic investigation of the effects of these properties on the performance of ZIF based sensors would promote the further development in sensing applications such as array-based sensing

M. Tu, S. Wannapaiboon, Dr. K. Khaletskaya, Prof. R. A. Fischer
Chair of Inorganic Chemistry II-Organometallics and Materials Chemistry
Ruhr-Universität Bochum
D-44780 Bochum, Germany
E-mail: roland.fischer@rub.de

DOI: 10.1002/adfm.201500760

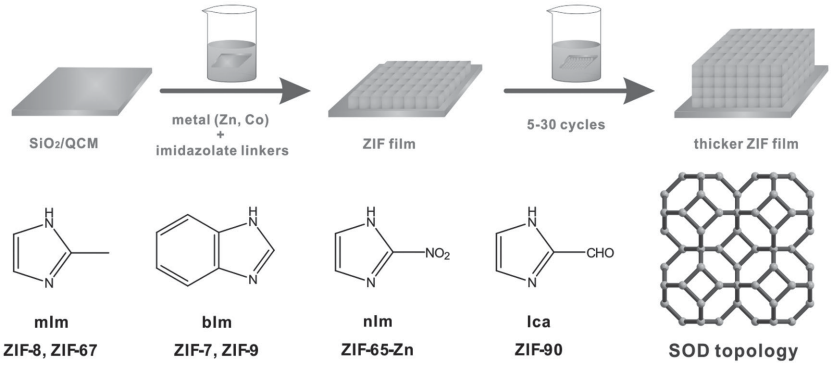

Figure 1. Schemes of repeated direct growth of ZIF thin films on SiO_2 surface (top) and the imidazolate linkers in the frameworks of ZIFs with SOD topology (down).

technology. However, up to now, only a limited number of ZIF sensing devices has been proposed. Herein we demonstrate the extension of the repeated direct growth technique to fabricate other functional ZIF thin films and the effects of the ZIF properties on the sensing performances are studied.

Thin films of sodalite-type (SOD) ZIFs (ZIF-7, 8, 9, 67, 90, and ZIF-65-Zn) with different metal centers (Zn and Co) and functional organic moieties were fabricated on SiO_2 coated QCM substrates for the detection of vapor phase volatile organic compounds (VOCs) at room temperature (**Figure 1**). All of these ZIFs are of SOD zeolite-type topology with large cavities interconnected via hexagonal small pore windows. Specifically, ZIF-7[27] and ZIF-9[19] are crystallized in trigonal space group using benzimidazole (bIm) as a linker but combining with different metal centers (Zn and Co, respectively). As the bulky linker bIm in the framework, the pore aperture of them is calculated to be 0.29 nm. ZIF-8[28] and ZIF-67[19] have a cubic structure owning the same organic linker, 2-methyimidazole (mIm), connected with Zn and Co, respectively. ZIF-65-Zn[29] and ZIF-90[30] are crystallized in cubic space group as well, however are constructed by the coordination bonds of Zn with 2-nitroimidazole (nIm) and imidazolate-2-carboxyaldehyde (Ica), respectively. The molecular sizes of the linkers (mIm, nIm, and Ica) in these four ZIFs are similar, leading to the similar pore opening (0.34 nm). These ZIFs have previously shown great potentials in many applications including CO_2 capture,[20] separation,[31–33] catalysis,[34] biomedicine,[35] and electrical devices.[36] However, only few of them are used as host materials for chemical sensing,[25,26] probably because of the high challenge of integrating them into signal transduction devices. The repeated direct growth method has shown its efficiency, but rather requires the rapid formation of ZIFs at room or relatively low temperature which is rarely explored and remains great challenges. Thus, we developed the simple protocols which enable the rapid room temperature formation of ZIFs. These simple protocols took advantage for repeated direct growth of uniform, dense, and continuous ZIF thin films on SiO_2 coated QCM substrates. Moreover, the developed automatic program controlled growth technique for ZIF film growth is easy to operate and allows scale up with high reproducibility compared to previous reported manual growth protocols. Compared to the growth of MOFs on self-assembly monolayer (SAM) modified gold substrate, the direct growth of MOFs on SiO_2 surface is able to form such strong covalent bond, providing more thermally stable interface.[37]

In order to systematically investigate the influence of ZIF functionalities on the sensing performances of ZIF/QCM devices, a series of analytes (including polar alcohol and water molecules, nonpolar hexane isomers with different molecular shapes and sizes, and aromatic BTEX compounds (benzene, toluene, ethylbenzene (EB), and xylene isomers (para-xylene (PX), ortho-xylene (OX), and meta-xylene (MX))) were chosen for the chemical detection measurements. The physical properties of these VOCs are summarized in Table S1 (Supporting Information). Taking advantages of the uniform ZIF thin films as well as the QCM technique, we systematically investigated the effects of ZIF pore size, LPD, surface functionality, and structural flexibility on the sensing performances of ZIF/QCM devices. Furthermore, since the QCM responses are directly related to mass changes of ZIF films, the observed selective adsorption phenomenon are discussed in relation to some valuable industrial separation cases including biofuel recovery and separation of benzene/cyclohexane, xylene, and hexane isomers.

2. Results and Discussion

2.1. Fabrication and Characterization of ZIF Thin Films

ZIF thin films deposited on various surfaces were previously reported by several different methods including direct growth,[25] layer-by-layer,[38] solvothermal,[39,40] and seeded growth.[32] Among them, the direct growth approach has shown its feasibility in rapid room temperature fabrication of uniform, dense, and continuous ZIF thin films with tunable thickness.[25,41] However, only ZIF-8 thin film was reported by this method up to date, because the requirement of rapid formation of ZIF materials at room temperature limits the extension to other ZIF thin films. We herein developed simple protocols for the rapid syntheses of these ZIFs at room temperature, which would benefit for the fabrication of ZIF thin films utilizing the repeated direct growth. In general, by carefully choosing the metal source and solvent, these ZIFs can be simply formed by mixing the metal source and imidazolate linker solutions at room temperature for 30–60 min. The details of rapid room temperature syntheses of these ZIFs are given in the Supporting Information. As shown in Figures S3–S8 (Supporting Information), all the powder X-ray diffraction (PXRD) patterns of as-synthesized ZIFs match the calculated corresponding patterns, demonstrating the successful syntheses of these ZIFs by this straightforward method.

The feasibility of rapid syntheses of these ZIFs at room temperature encouraged us to grow them as thin films using the repeated direct growth method. We developed the setup (shown in Figure S1, Supporting Information) to fulfill the repeated direct growth with automatic program control which is much

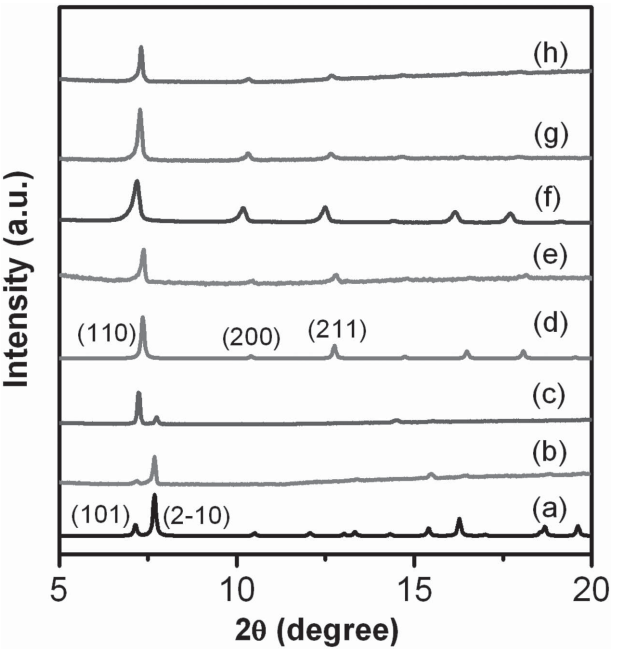

Figure 2. XRD patterns of ZIF thin films grown on SiO_2 surface with ten deposition cycles in comparison with calculated ZIF-7 and ZIF-8, respectively: a) calculated bulk ZIF-7 (trigonal); b) ZIF-7; c) ZIF-9; d) calculated bulk ZIF-8 (cubic); e) ZIF-8; f) ZIF-65-Zn; g) ZIF-67; h) ZIF-90.

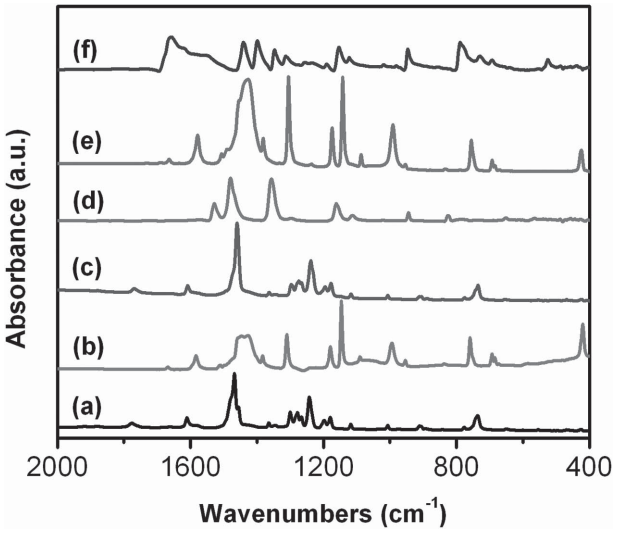

Figure 3. IRRA spectra of ZIF thin films grown on SiO_2 surface with ten deposition cycles: a) ZIF-7; b) ZIF-8; c) ZIF-9; d) ZIF-65-Zn; e) ZIF-67; and f) ZIF-90.

easier to handle compared to the previous manual coating procedure.[25] The X-ray diffraction (XRD) patterns of as-prepared ZIF films in comparison with corresponding calculated patterns shown in **Figure 2** clearly demonstrate the successful fabrication of these ZIF structures on the substrates without impure phases. In addition, as shown in Figures S9–S14 (Supporting Information), more growth cycles give rise to higher reflection intensity, indicating the increase of film thickness.

The infrared reflection absorption (IRRA) spectrum of each ZIF thin film in comparison with the spectrum of the corresponding bulk powder ZIF confirms that the chemical bond structures of these ZIF films are in accordance with the reported ZIFs (Figures S15–S20, Supporting Information). The IRRA spectra of these ZIF films with 10 deposition cycles are shown in **Figure 3**. The absorption band at 740 cm^{-1} in the spectra of ZIF-7 and ZIF-9 is associated with the typical out-of-plane C–H bending vibration of ortho-disubstituted benzene which is contributed from bIm ligand. The spectrum of ZIF-65-Zn possesses the typical symmetric and asymmetric stretching vibration of nitro-group at 1350 and 1520 cm^{-1}, respectively. The vibration observed at 1665 cm^{-1} in ZIF-90 spectrum is associated with the asymmetric vibration of C=O of Ica linker.

The morphologies of ZIF films were inspected by scanning electron microscope (SEM). The SEM images of ZIF-7, 8, 9, 67, 90, and ZIF-65-Zn films with 10 growth cycles are shown in **Figure 4**. The surfaces of all the obtained ZIF films are continuously uniform without visible cracks and defects, which is feasible for chemical detection. The cross section views of ZIF films with different number of deposition cycles shown in Figures S21–S26 (Supporting Information) suggest the controllable thickness by varying the number of growth cycles. In addition, the thicknesses of these ZIF films with 10 growth cycles are less than 1 μm. It is suitable for the application in QCM sensing since the thickness as high as several micrometers would result in low or no response of QCM device upon exposure to guest molecules. The SEM images together with the XRD patterns demonstrate that the repeated direct growth method is one promising technique for the fabrication

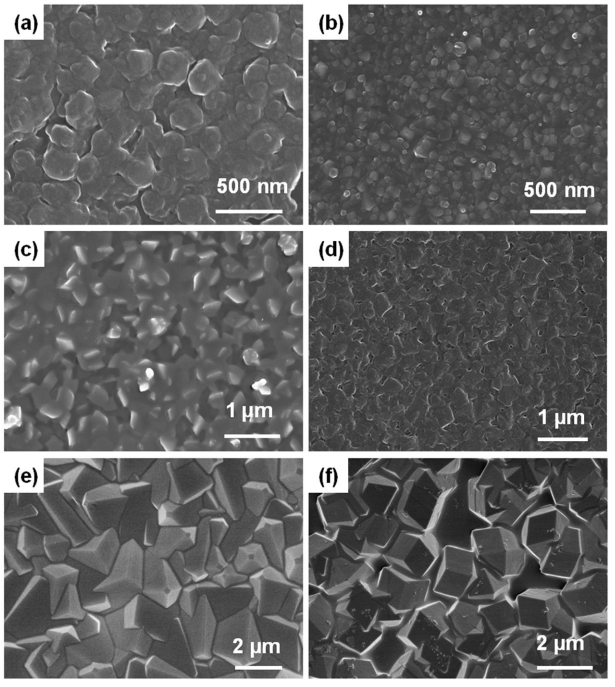

Figure 4. SEM images of ZIF thin films grown on SiO_2 surface with ten growth cycles: a) ZIF-7; b) ZIF-8; c) ZIF-9; d) ZIF-65-Zn; e) ZIF-67; and f) ZIF-90.

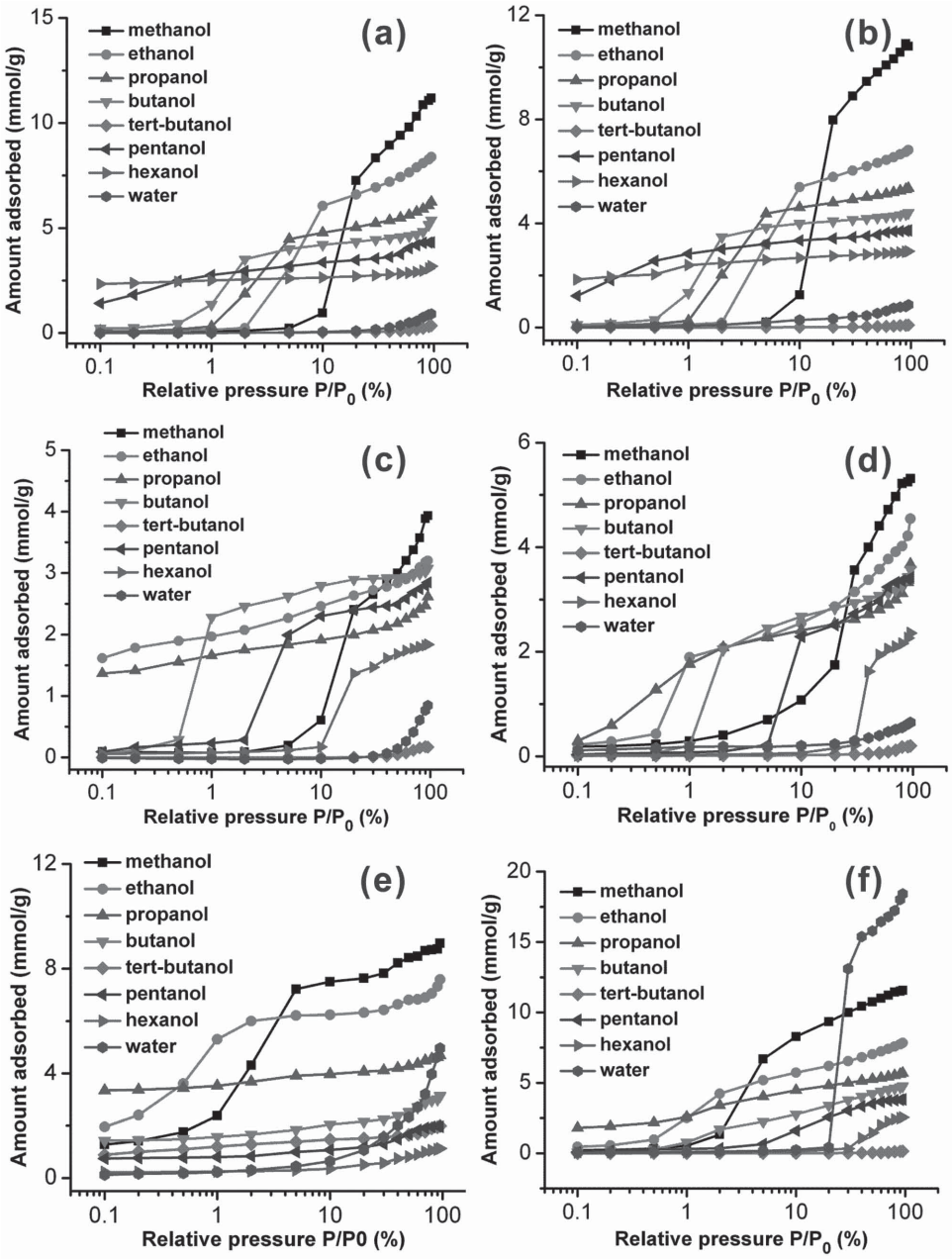

Figure 5. Adsorption isotherms of alcohols and water on ZIF/QCM devices at 293 K: a) ZIF-8; b) ZIF-67; c) ZIF-7; d) ZIF-9; e) ZIF-65-Zn; and f) ZIF-90.

of highly crystalline, homogeneous, and dense ZIF films with controllable thickness under mild conditions.

2.2. Detection of Alcohols and Water

As a prototypical ZIF, ZIF-8 has been well investigated in terms of the adsorption of alcohols and water in bulk powder case.[42,43] Therefore, we first performed the detection measurements on ZIF-8/QCM device to compare with the reported data. The adsorption isotherms of studied alcohols on ZIF-8/QCM device at 293 K are shown in **Figure 5**a. Except unreported isotherms (pentanol, hexanol, and *tert*-butanol), both the isotherm shapes and the saturated adsorption amount are similar to the previous reported data,[42,43] which confirms the high crystallinity of the ZIF-8 film as well as the feasibility of the QCM technique for chemical sensing applications. As shown in Figure 5a, all alcohols are detectable except *tert*-butanol of which the molecular size is too bulky to penetrate into the cage of ZIF-8. The detection limits of the primary alcohols depend on the carbon number (or the length) of the alkyl groups within the molecules, of which the detectable concentration decreases in the following order: methanol > ethanol > propanol > butanol > pentanol > hexanol. This phenomenon could be reasonably explained by the increase of hydrophobicity by extending the linear alkyl groups of the primary alcohols. According to the

hydrophobic feature of ZIF-8, the more hydrophobic the probe linear alcohols are, the lower concentration could be detected. Moreover, the typical type III water adsorption isotherm is observed with quite low uptake even at near saturated vapor pressure, which is also related to the strong hydrophobic feature of ZIF-8. The absence of hysteresis in the adsorption and desorption branches of alcohol sorption isotherms allows the adsorbed alcohols to be easily removed which would benefit for reversible sensing (Figure S29, Supporting Information).

The adsorption isotherms of studied alcohols and water on ZIF-7/QCM device are shown in Figure 5c. Similar to the detection performance of ZIF-8, water and *tert*-butanol cannot be detected because of the hydrophobic nature and LPD of ZIF-7. However, the hysteresis is observed in methanol sorption isotherms of ZIF-7 indicating the gate-opening sorption phenomenon (Figure S30, Supporting Information), which can be attributed to its high flexibility. The XRD investigations shown in **Figure 6** confirm the reversible structure transformation of ZIF-7 from its narrow pore phase to large pore phase upon loading and removal of methanol molecules.[44,45] Interestingly, the typical Langmuir type isotherms are observed instead of the gate-opening sorption behavior in the cases of ethanol and propanol sorption on ZIF-7/QCM device in spite of their larger molecular sizes compared to methanol. However, the XRD results (Figure 6) still indicate the reversible structural flexibility of ZIF-7 upon adsorption and desorption of ethanol and propanol. Therefore, we propose that the typical Langmuir type isotherms (without hysteresis) are attributed to the higher hydrophobicity of ethanol and propanol compared to methanol, which leads to the direct pore opening from its narrow pore phase to large pore phase at such a very low vapor pressure. In the case of detecting butanol, pentanol, and hexanol on ZIF-7/QCM device (Figure 5c and Figure S28, Supporting Information), the gate-opening sorption behavior (showing the hysteresis in adsorption–desorption curves) can be observed and the gate-opening pressure increases in the following sequence: butanol < pentanol < hexanol. This phenomenon is ascribed to the bigger molecular sizes of them which results in higher resistance to open the pore window, even though they are much more hydrophobic. To sum up, the gate-opening phenomena are observed in the cases that the probe alcohol molecules are rather small but less hydrophobic (e.g., methanol) as well as the molecules are highly hydrophobic but rather large (e.g., butanol). The similar sensing performances of alcohols and water can be observed on its cobalt analogue ZIF-9/QCM device (Figure 5d) except that the gate-opening pressure in each case is slightly higher. From this observation, it is possible to state that Zn-based ZIFs have higher flexibility compared to its Co analogue, which is similar to the pillar-layer MOFs of which the sorption behavior are different depending on the constructing metal centers.[46]

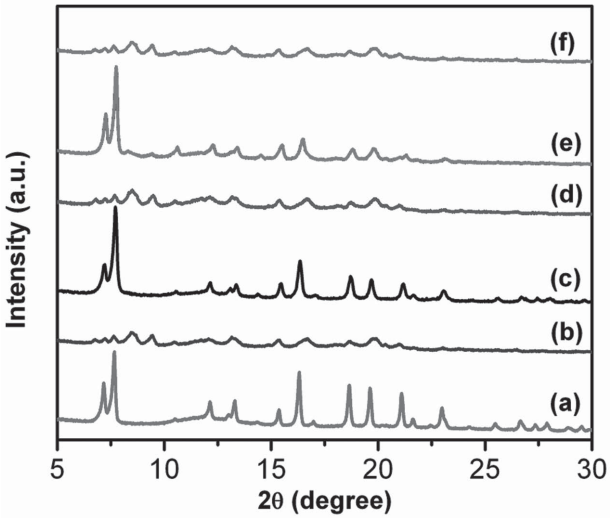

Figure 6. PXRD patterns of ZIF-7: a) as-synthesized; b) activated; c) loaded with methanol; d) removal of methanol; e) loaded with ethanol; f) removal of ethanol.

Due to the presence of polar moiety (nitro group), water molecules can be detected even at very low concentration on ZIF-65-Zn/QCM device (Figure 5e). Unlike its analogue ZIF-8, all the alcohols can be adsorbed even at very low concentration (0.1%). The XRD pattern of activated ZIF-65-Zn shows different pattern compared to the as-synthesized one, suggesting its flexibility upon removal of guest molecules (Figure S31, Supporting Information). Even though we cannot solve the structure of activated ZIF-65-Zn at this moment, the observed shift of [110] reflection to lower 2θ position suggests the bigger distance in [110] crystallographic direction, thus leads to larger pore opening in this direction compared to the as-synthesized one. As a result of the bigger pore aperture together with its hydrophilic nature, ZIF-65-Zn can readily adsorb all the studied alcohols even the biggest studied molecule *tert*-butanol at very low vapor pressure. Unlike the reversible flexibility of ZIF-7, the structural change of ZIF-65-Zn is irreversible after removal of solvents. As shown in Figure S31 (Supporting Information), the structure of activated ZIF-65-Zn does not change upon loading of guest alcohol molecules. In the case of ZIF-90/QCM device, water molecules cannot be detected until the relative pressure (20%), and large uptake of water is observed at high relative pressure due to the existence of hydrophilic carboxaldehyde group in the framework (Figure 5f).

These SOD ZIF/QCM hybrid devices exhibit different selective sensing performances upon exposure to different alcohol and water vapors due to their differences on surface hydrophobicity, LPD, structure flexibility, as well as the different physical properties of analytes. As one type of renewable energy, bioalcohols such as bioethanol and biobutanol have the potential to reduce the dependence on petroleum based energy sources.[47] However, the major challenge in the production of bioalcohols as fuel-grade alcohols is the efficient recovery of them from their aqueous medium. ZIF-8 has been investigated for the biobutanol separation from its aqueous medium.[42] The high uptake of ethanol and butanol at much lower vapor pressure indicates that ZIF-7 may be superior to ZIF-8 in the potential for bioethanol and biobutanol extraction.

2.3. Detection of BTEX Compounds and Cyclohexane

As a typical class of VOCs, BTEX compound obtained as a mixture in the refining of crude oil can result in significant widespread emissions to the environment. The most important

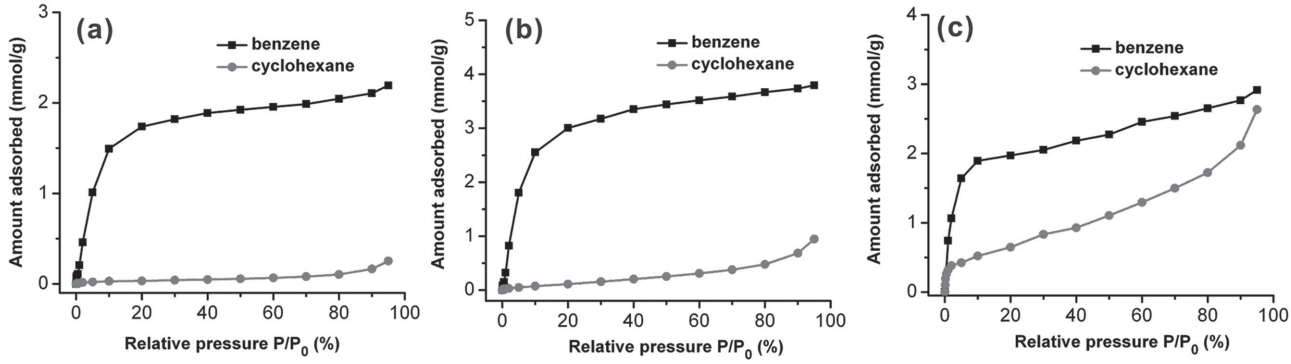

Figure 7. Adsorption isotherms of benzene and cyclohexane on ZIF/QCM devices at 293 K: a) ZIF-7, b) ZIF-8; and c) ZIF-65-Zn.

source of human exposure to BTEX compounds is from the breathing of contaminated air. Thus, it is necessary to built sensors for real-time monitoring them. Moreover, the selective detection and separation of benzene/cyclohexane and xylene isomers is among the most important and most difficult processes in petrochemistry due to their high importance for further valuable products and their similar boiling points and molecular sizes (Table S1, Supporting Information).[48,49] Thus, the adsorption of vapor phase BTEX compounds and cyclohexane on obtained ZIF/QCM devices were systematically investigated.

Despite of the large molecular size of benzene compared to the LPD of ZIF-7 and ZIF-8, it can be readily adsorbed in the pores (**Figure 7**), which can be ascribed to the hexagonal window opening induced by strong host–guest interactions (π–π interaction) between benzene molecules and the imidazolate linkers. By contrast, cyclohexane cannot be adsorbed at all due to the absence of strong interaction, even though it has similar molecular size to benzene. All the obtained ZIF/QCM devices have the selective adsorption of benzene over cyclohexane except ZIF-65-Zn (Figure 7 and Figure S30, Supporting Information), which can also confirm that the LPD of ZIF-65-Zn becomes larger after activation allowing cyclohexane to transport into its pores.

The adsorption isotherms of xylene isomers and EB on ZIF-8/QCM devices show selective detection of PX and EB over MX and OX due to the shape selective adsorption (**Figure 8**b). Interestingly, even though the LPD and pore size of ZIF-7 is much smaller than ZIF-8 resulting no N_2 adsorption even at room temperature, EB, MX, and OX can be adsorbed with gate-opening phenomenon. Even in the presence of strong π–π interaction between these molecules and ZIF-7 framework, their molecular sizes are too large to open the pore window of ZIF-7 at low pressure. With the increase of concentration, the higher vapor pressure could result in the pore opening as well as structure transformation to allow these molecules penetrating into the cages. However, the PX isotherm does not show gate-opening behavior, and exhibits lower adsorption amount compared to EB, MX, and OX, even though the size of PX is the smallest one. Thus, we performed XRD investigation on ZIF-7 upon loading of these guest molecules. As shown in **Figure 9**, after loading with EB, MX, and OX, the structure of ZIF-7 transforms from its narrow pore phase to its large pore phase.[44] However, the structure of ZIF-7 transforms to another unknown phase upon the adsorption of PX. Thus, we speculate that the pore volume of the new phase induced by the adsorption of PX is in between its narrow and large pore, resulting in lower uptake of PX. Moreover, the large pore phase of ZIF-7 can transform to its narrow pore phase after removal of the BTEX compounds, demonstrating the reversible flexibility of ZIF-7 upon adsorption and desorption of guest molecules (Figure S38, Supporting Information). As the cobalt analogue of ZIF-7, ZIF-9 shows the similar detection performances of BTEX compounds except the higher gate-opening pressure in each case (Figure S33, Supporting Information), probably due to the lower flexibility as discussed in the

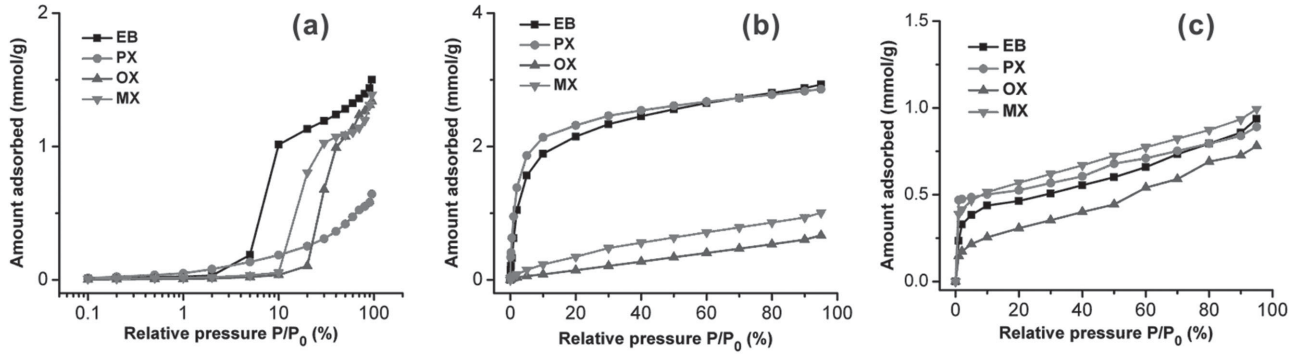

Figure 8. Adsorption isotherms of xylene isomers (para-xylene (PX), ortho-xylene (OX), and meta-xylene (MX)) and ethylbenzene (EB) on ZIF/QCM devices at 293 K: a) ZIF-7; b) ZIF-8; c) ZIF-65-Zn.

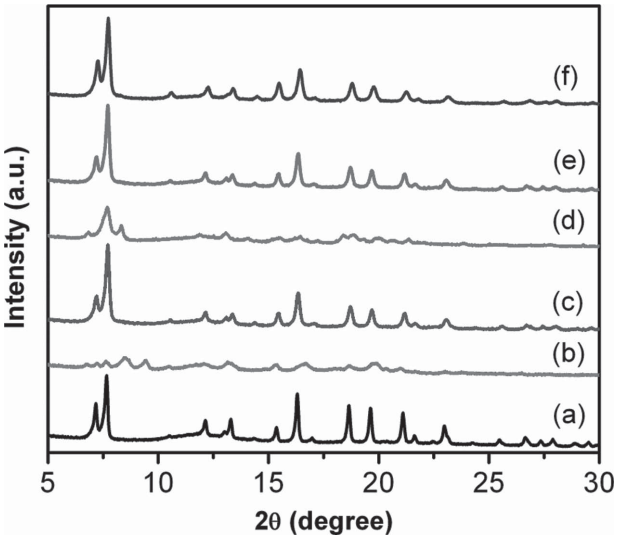

Figure 9. PXRD patterns of ZIF-7: a) as-synthesized; b) activated; c) loaded with EB; d) loaded with PX; e) loaded with MX; f) loaded with OX.

aforementioned section. The different gate-opening pressures in the cases of adsorption of xylene isomers and EB on ZIF-7 and ZIF-9 may be beneficial for further study to achieve the efficient separation of them by pressure swing adsorption (PSA) cycles. ZIF-67 and ZIF-90/QCM devices also exhibit selective detection of xylene isomers and EB (Figure S33, Supporting Information), while no significant selective adsorption could be observed on ZIF-65-Zn/QCM device due to the existence of larger LPD.

Due to their differences on LPD and structure flexibility, the SOD ZIF/QCM devices show different selective detection performances on BTEX compounds and cyclohexane. Thus, selective detection in the mixture of these components may be achieved by array-based sensing technique. The selective adsorption of xylene isomers and EB suggests these SOD ZIFs may serve as good candidates for further study to achieve the challenge on the efficient separation of them. The observed selective adsorption of benzene over cyclohexane at the entire concentration on these SOD ZIFs except ZIF-65-Zn suggests that they may be useful for separation of benzene/cyclohexane by adsorptive separation or membrane pervaporation techniques.

2.4. Detection of Hexane Isomers

Hexanes are generated through a catalytic isomerization reaction, consist of an equilibrium distribution of unreacted n-hexane (referred as hexane), monobranched isomers 2-methylpentane (2-MP), 3-methylpentane (3-MP), and dibranched isomers 2,3-dimethylbutane (2,3-DMB) and 2,2-dimethylbutane (2,2-DMB). The value of a particular isomer as a component in the gasoline is related to its research octane number (RON) which increases with the degree of branching: hexane = 30; 2-MP = 45; 3-MP = 75.5; 2,2-DMB = 94; 2,3-DMB = 105.[50] Therefore, dibranched isomers are preferred

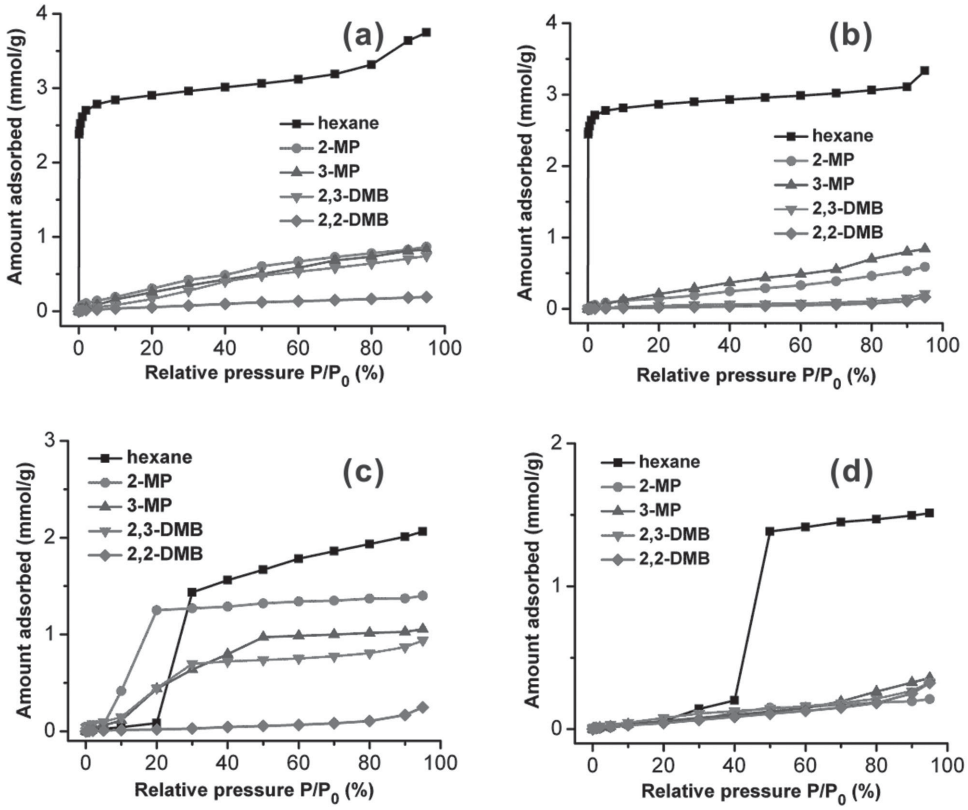

Figure 10. Adsorption isotherms of hexane isomers on ZIF/QCM devices at 293 K: a) ZIF-8; b) ZIF-67; c) ZIF-7; d) ZIF-9.

products in an isomerization process. Considering that SOD ZIFs own the sodalite zeolite topology with large cages interconnected by small pore window, it is interesting to investigate the efficiency of them for hexane isomer separation by shape selective adsorption.

Herein, we measured the adsorption of hexane isomers on the SOD ZIF/QCM devices. As shown in **Figure 10**a, a large amount of hexane can be adsorbed on ZIF-8, while no detection of 2,2-DMB can be observed even at the high concentration due to its largest molecular size among the five hexane isomers. 2-MP, 3-MP, and 2,3-DMB can also be detected but with much lower saturated adsorption amount compared to hexane. As the cobalt analogue of ZIF-8, ZIF-67 also shows high uptake of hexane and size exclusion of 2,2-DMB (Figure 10b). However, 2,3-DMB cannot be detected at the entire concentration, which can be attributed to its lower flexibility of ZIF-67 that 2,3-DMB is not able to open the window for passing through. The selective adsorption of n-hexane and monobranched hexane over dimer-branched hexane indicates that ZIF-67 can be used for removal of n-hexane and monobranched hexane from the mixture of hexane isomers, leading to gasoline RON enhancement. The adsorption isotherms of hexane isomers on ZIF-7/QCM device are shown in Figure 10c. The typical gate-opening sorption behaviors of hexane, 2-MP, 3-MP, and 2,3-DMB are observed, which also confirm the flexibility of ZIF-7. Similar to the case of ZIF-8, 2,2-DMB cannot be adsorbed due to the steric exclusion effect. ZIF-9/QCM device only shows gate-opening adsorption behavior upon detection of hexane, and the gate-opening pressure is higher than on ZIF-7. This phenomenon together with the non-adsorption of other 4 isomers can also confirm the above conclusion that the cobalt ZIF owns lower flexibility compared to its zinc analogue.

From the single component adsorption isotherms of hexane isomers on the SOD ZIF/QCM devices, we can observe that hexane can be adsorbed with high uptakes, while 2,2-DMB cannot be adsorbed except low uptake on ZIF-65-Zn (Figure S34, Supporting Information). It suggests that these SOD ZIFs may have the potential for separation of hexane isomers to enhance the gasoline RON. Particularly, the selective adsorption of hexane and monobranched hexane over dibranched hexane indicates that ZIF-67 is superior to other SOD ZIFs for hexane isomers separation due to its lower structure flexibility.

2.5. Stability Tests

In the application of chemical detection as well as separation, the humidity stability is an important issue. Hence, we performed three cycles' water-methanol repetition measurements on these SOD ZIF/QCM devices. As shown in Figure S39 (Supporting Information), except ZIF-65-Zn/QCM device, neither the shape nor the saturated adsorption amount in the methanol and water adsorption isotherms of all the ZIF/QCM devices change significantly, indicating their stability over humidity. More importantly, after the exposure to the ambient air for three months, the methanol adsorption isotherms (both the shape and saturated uptake) of these ZIF/QCM devices keep almost the same, except ZIF-65-Zn. These stability tests suggest high stability of these SOD ZIF/QCM devices against moisture and air, which is important for the realistic application of them.

3. Conclusions

In summary, we developed convenient methods for rapid room temperature formation of SOD ZIFs, which were utilized for growth of ZIF thin films coupling repeated direct growth method in an automatic operation. The fabricated ZIF thin films are highly crystalline, uniform, dense, and continuous with controllable thickness. Taking advantages of QCM technique, the SOD ZIF thin films fabricated on SiO_2 coated QCM substrates were systematically investigated for selective detection of various VOC vapors. Due to their differences on LPD, hydrophobicity, structure flexibility, and the different physical properties of studied analytes, these ZIF/QCM devices exhibit different selective detection behaviors on vapor phase alcohol/water, BTEX compounds, and hexane isomers. For instance, several primary alcohols can be detected on ZIF-7, 8, 9, and 67, while no detection of water vapor could be observed on them due to their high hydrophobicity. However, because of the presence of polar moieties in the framework of ZIF-90 and ZIF-65-Zn, water molecules could be detected at different humilities. The selective single component adsorption of studied VOC vapors on these SOD ZIF/QCM hybrid devices provides the evidence that selective detection of different chemicals in the mix-components environment could be achieved by array-based sensing techniques using a number of different ZIF/QCM devices. Furthermore, according to the observed selective adsorption phenomenon, these ZIFs may serve as good candidates for biofuel recovery and the separation of benzene/cyclohexane, xylene, and hexane isomers which are important and still remain challenges in industry. Finally, the above mentioned stability tests on these ZIF/QCM devices suggest the possibility to employ them into realistic applications.

4. Experimental Section

Fabrication of ZIF Thin Film Devices: ZIF thin films were fabricated on SiO_2 (50 nm) coated Si wafers (typically 1 cm × 1 cm) or commercial SiO_2 coated QCM substrates (AT-cut, 5 MHz, q-sense). The substrates were pretreated by subsequently immersing in acetone and ethanol under sonication for 30 min and then dried under argon. Before the deposition of ZIF films, the substrates were activated in the UV ozone chamber for 1 h to remove the organic contaminants and increase –OH groups on the surfaces. The ZIF thin films were deposited by automatic pump controlled process as shown in Figure S1 (Supporting Information). The pretreated substrate was fixed on a home-made teflon sample holder and placed into the deposition cell in a face-down-to-bottom fashion. Then the metal and linker solutions were simultaneously dosed to the sample cell to grow the ZIF film on the substrate. After a certain time (30–60 min), the mixed solution was removed from the growth cell. Before starting the next deposition cycle, the substrate was washed with methanol (10 min) and dried under the atmosphere (10 min). Thin films with different thicknesses can be obtained by repeating this procedure with different number of cycles (5–30 in this work). The optimized metal source, solvent, precursor concentration as well as deposition time are different in each case. The detailed fabrication parameters for these ZIF film devices are given in the Supporting Information.

General Methods: XRD data of ZIF thin films were collected by the X'Pert PRO PANanalytical equipment (Bragg–Brentano geometry with automatic divergence slits, position sensitive detector, continuous mode, room temperature, Cu-Kα radiation, Ni filter, the range of $2\theta = 5°–20°$, at a step of 0.0197°, with accumulation time 550 s per step). The powder samples were dropped onto a zero background silicon wafer, and measured at the same equipment (5°–30°, at a step of 0.0197°, with accumulation time 200 s per step). Infrared (IR) spectra of powders were recorded inside a glovebox on a Bruker Alpha-P FTIR instrument in the attenuated total reflection (ATR) geometry with a diamond ATR unit. IRRA spectroscopy measurements were done on a Biorad Excalibur FTIR spectrometer (FTS 3000) with 2 cm^{-1} resolution at an angle of incidence of 80° relative to the surface normal and further processed by using boxcar apodization. SEM images were recorded on a LEO1530 Gemini FESEM or FEI ESEM Dual Beam Quanta 3D FEG microscope to investigate the surface morphologies and thicknesses of ZIF films.

Detection of Vapor Phase VOCs on ZIF/QCM Devices: The detection of vapor phase VOCs on ZIF/QCM devices were performed on an environment controlled QCM equipment. As shown in Figure S2 (Supporting Information), the relative vapor pressure of analytes could be controlled by four independent mass flow controllers (MFCs) in the range of 0%–95%. Quantitative mass change of ZIF films mounted on QCM substrate was obtained from the frequency change according to the Sauerbrey equation[51] (shown in Equation (1), where ΔM is the mass change on the ZIF/QCM device; F_0 is the fundamental frequency of blank QCM substrate; A is the surface area of electrode; μ is Shear stress of quartz (2.947×10^{10} kg/(m × s^2)); ρ is the density of quartz (2648 kg m^{-3}); ΔF is the frequency change. In the case of the QCM substrate we used in this work ($F_0 \approx 5$ MHz), mass detection sensitivity calculated by Equation (1) becomes 17.7 ng cm^{-2} at the resolution of 1 Hz.

$$\Delta M = -\frac{A\sqrt{\mu \times \rho}}{2F_0^2}\Delta F \quad (1)$$

At each relative pressure, the adsorption amount (normalized in g/g) could be obtained by Equation (2), where M_0 is the mass of the ZIF thin film on QCM substrate; F is the equilibrium frequency; F_s is the frequency of ZIF/QCM device after pretreatment of the sample

$$\frac{\Delta M}{M_0} = \frac{F - F_s}{F_s - F_0} \quad (2)$$

Prior to the detection of vapor phase VOCs, it is important to remove all solvent molecules from the pores to be able to compare the sorption data of different ZIF/QCM devices. The activation process was performed in two steps. First, ZIF/QCM devices were soaked in absolute CH_2Cl_2 at least overnight at room temperature and subsequently dried in a He stream. Additionally, they were placed into the QCM instrument cells and heated at 80 °C under He stream (99.999%, 100 sccm) for 2 h. As monitoring the frequency change during the pretreatment, the frequency could reach equilibrium in 2 h activation at 80 °C, indicating the complete removal of guest molecules. All the detection measurements were performed at 293 K. The equilibrium time was set to be 30 min and the ΔF was set in the range of ±5 Hz.

Supporting Information

Supporting Information is available from the Wiley Online Library or from the author.

Acknowledgements

This work was funded within the Priority Program 1362 "Metal-Organic Frameworks" of the German Research Foundation (DFG). M.T. is grateful for a PhD fellowship from the China Scholarship Council (CSC). S.W. is grateful for PhD scholarship from the Royal Thai Government under the Ministry of Science and Technology.

Received: February 25, 2015
Revised: May 15, 2015
Published online: June 12, 2015

[1] L. E. Kreno, K. Leong, O. K. Farha, M. Allendorf, R. P. Van Duyne, J. T. Hupp, *Chem. Rev.* **2012**, *112*, 1105.
[2] B. Liu, *J. Mater. Chem.* **2012**, *22*, 10094.
[3] Z. Hu, B. J. Deibert, J. Li, *Chem. Soc. Rev.* **2014**, *43*, 5815.
[4] S. R. Batten, N. R. Champness, X.-M. Chen, J. Garcia-Martinez, S. Kitagawa, L. Öhrström, M. O'Keeffe, M. P. Suh, J. Reedijk, *Pure Appl. Chem.* **2013**, *85*, 1715.
[5] S. Achmann, G. Hagen, J. Kita, I. Malkowsky, C. Kiener, R. Moos, *Sensors* **2009**, *9*, 1574.
[6] M. D. Allendorf, A. Schwartzberg, V. Stavila, A. A. Talin, *Chem. Eur. J.* **2011**, *17*, 11372.
[7] M. Tu, S. Wannapaiboon, R. A. Fischer, *Inorg. Chem. Front.* **2014**, *1*, 442.
[8] V. Stavila, A. A. Talin, M. D. Allendorf, *Chem. Soc. Rev.* **2014**, *43*, 5994.
[9] K. Okada, R. Ricco, Y. Tokudome, M. J. Styles, A. J. Hill, M. Takahashi, P. Falcaro, *Adv. Funct. Mater.* **2014**, *24*, 1969.
[10] P. Falcaro, R. Ricco, C. M. Doherty, K. Liang, A. J. Hill, M. J. Styles, *Chem. Soc. Rev.* **2014**, *43*, 5513.
[11] C. M. Doherty, G. Grenci, R. Riccò, J. I. Mardel, J. Reboul, S. Furukawa, S. Kitagawa, A. J. Hill, P. Falcaro, *Adv. Mater.* **2013**, *25*, 4701.
[12] T. Yamada, K. Otsubo, R. Makiura, H. Kitagawa, *Chem. Soc. Rev.* **2013**, *42*, 6655.
[13] S. K. Vashist, P. Vashist, *J. Sensors* **2011**, *2011*, 13.
[14] E. Biemmi, A. Darga, N. Stock, T. Bein, *Microporous Mesoporous Mater.* **2008**, *114*, 380.
[15] H. Uehara, S. Diring, S. Furukawa, Z. Kalay, M. Tsotsalas, M. Nakahama, K. Hirai, M. Kondo, O. Sakata, S. Kitagawa, *J. Am. Chem. Soc.* **2011**, *133*, 11932.
[16] B. Liu, M. Tu, D. Zacher, R. A. Fischer, *Adv.Funct. Mater.* **2013**, *23*, 3790.
[17] M. Tu, R. A. Fischer, *J. Mater. Chem. A* **2014**, *2*, 2018.
[18] S. Wannapaiboon, M. Tu, R. A. Fischer, *Adv. Funct. Mater.* **2014**, *24*, 2696.
[19] K. S. Park, Z. Ni, A. P. Côté, J. Y. Choi, R. Huang, F. J. Uribe-Romo, H. K. Chae, M. O'Keeffe, O. M. Yaghi, *Proc. Natl. Acad. Sci. U.S.A.* **2006**, *103*, 10186.
[20] R. Banerjee, A. Phan, B. Wang, C. Knobler, H. Furukawa, M. O'Keeffe, O. M. Yaghi, *Science* **2008**, *319*, 939.
[21] J.-P. Zhang, Y.-B. Zhang, J.-B. Lin, X.-M. Chen, *Chem. Rev.* **2012**, *112*, 1001.
[22] J. Yao, H. Wang, *Chem. Soc. Rev.* **2014**, *43*, 4470.
[23] Y. Hwang, H. Sohn, A. Phan, O. M. Yaghi, R. N. Candler, *Nano Lett.* **2013**, *13*, 5271.
[24] E.-X. Chen, H. Yang, J. Zhang, *Inorg. Chem.* **2014**, *53*, 5411.
[25] G. Lu, J. T. Hupp, *J. Am. Chem. Soc.* **2010**, *132*, 7832.
[26] S. Liu, Z. Xiang, Z. Hu, X. Zheng, D. Cao, *J. Mater. Chem.* **2011**, *21*, 6649.
[27] X. Huang, J. Zhang, X. Chen, *Chin. Sci. Bull.* **2003**, *48*, 1531.
[28] X.-C. Huang, Y.-Y. Lin, J.-P. Zhang, X.-M. Chen, *Angew. Chem. Int. Ed.* **2006**, *45*, 1557.
[29] C. Dey, R. Banerjee, *Chem. Commun.* **2013**, *49*, 6617.
[30] W. Morris, C. J. Doonan, H. Furukawa, R. Banerjee, O. M. Yaghi, *J. Am. Chem. Soc.* **2008**, *130*, 12626.

[31] J. van den Bergh, C. Gücüyener, E. A. Pidko, E. J. M. Hensen, J. Gascon, F. Kapteijn, *Chem. Eur. J.* **2011**, *17*, 8832.
[32] Y.-S. Li, F.-Y. Liang, H. Bux, A. Feldhoff, W.-S. Yang, J. Caro, *Angew. Chem. Int. Ed.* **2010**, *49*, 548.
[33] A. Huang, W. Dou, J. Caro, *J. Am. Chem. Soc.* **2010**, *132*, 15562.
[34] H.-L. Jiang, B. Liu, T. Akita, M. Haruta, H. Sakurai, Q. Xu, *J. Am. Chem. Soc.* **2009**, *131*, 11302.
[35] S. Diring, D. O. Wang, C. Kim, M. Kondo, Y. Chen, S. Kitagawa, K.-I. Kamei, S. Furukawa, *Nat. Commun.* **2013**, *4*, 2684.
[36] S. Eslava, L. Zhang, S. Esconjauregui, J. Yang, K. Vanstreels, M. R. Baklanov, E. Saiz, *Chem. Mater.* **2012**, *25*, 27.
[37] A. L. Robinson, V. Stavila, T. R. Zeitler, M. I. White, S. M. Thornberg, J. A. Greathouse, M. D. Allendorf, *Anal. Chem.* **2012**, *84*, 7043.
[38] O. Shekhah, M. Eddaoudi, *Chem. Commun.* **2013**, *49*, 10079.
[39] X. Zhang, Y. Liu, S. Li, L. Kong, H. Liu, Y. Li, W. Han, K. L. Yeung, W. Zhu, W. Yang, J. Qiu, *Chem. Mater.* **2014**, *26*, 1975.
[40] K. Khaletskaya, S. Turner, M. Tu, S. Wannapaiboon, A. Schneemann, R. Meyer, A. Ludwig, G. Van Tendeloo, R. A. Fischer, *Adv. Funct. Mater.* **2014**, *24*, 4804.
[41] G. Lu, O. K. Farha, W. Zhang, F. Huo, J. T. Hupp, *Adv. Mater.* **2012**, *24*, 3970.
[42] J. C. S. Remi, T. Rémy, V. Van Hunskerken, S. van de Perre, T. Duerinck, M. Maes, D. De Vos, E. Gobechiya, C. E. A. Kirschhock, G. V. Baron, J. F. M. Denayer, *ChemSusChem* **2011**, *4*, 1074.
[43] K. Zhang, R. P. Lively, M. E. Dose, A. J. Brown, C. Zhang, J. Chung, S. Nair, W. J. Koros, R. R. Chance, *Chem. Commun.* **2013**, *49*, 3245.
[44] S. Aguado, G. Bergeret, M. P. Titus, V. Moizan, C. Nieto-Draghi, N. Bats, D. Farrusseng, *New J. Chem.* **2011**, *35*, 546.
[45] P. Zhao, G. I. Lampronti, G. O. Lloyd, M. T. Wharmby, S. Facq, A. K. Cheetham, S. A. T. Redfern, *Chem. Mater.* **2014**, *26*, 1767.
[46] S. Bureekaew, S. Amirjalayer, R. Schmid, *J. Mater. Chem.* **2012**, *22*, 10249.
[47] D. Antoni, V. Zverlov, W. Schwarz, *Appl. Microbiol. Biotechnol.* **2007**, *77*, 23.
[48] Z. R. Herm, E. D. Bloch, J. R. Long, *Chem. Mater.* **2014**, *26*, 323.
[49] J. P. G. Villaluenga, A. Tabe-Mohammadi, *Membrane Sci.* **2000**, *169*, 159.
[50] Z. R. Herm, B. M. Wiers, J. A. Mason, J. M. van Baten, M. R. Hudson, P. Zajdel, C. M. Brown, N. Masciocchi, R. Krishna, J. R. Long, *Science* **2013**, *340*, 960.
[51] G. Z. Sauerbrey, *Physik* **1959**, *155*, 206.